

UNIVERSITA' DEGLI STUDI DI PADOVA
Dipartimento di Fisica e Astronomia *Galileo Galilei*

Corso di Laurea in Fisica

Study of the ion temperature dynamics in thermonuclear plasmas produced in the RFX-mod experiment

Laureando:
Stefano Milanese
Matricola:
1053440

Relatore:
Dott. Matteo Zuin
Correlatori:
Dott. Emilio Martines
Dott. Luigi Cordaro

Anno Accademico 2015-2016

Sommario

Questo lavoro di tesi é dedicato allo studio della dinamica della temperatura ionica in plasmi di interesse termonucleare a confinamento magnetico prodotti nell'esperimento RFX-mod. La configurazione magnetica di confinamento del plasma presa in considerazione é la cosiddetta Reversed Field Pinch (RFP), in cui la direzione del campo magnetico toroidale \mathbf{B}_ϕ viene rovesciata in prossimitá del bordo della camera in cui il plasma viene contenuto. In tale configurazione, in corrispondenza di valori razionali per il fattore di sicurezza $q(r) = \frac{rB_\phi}{RB_\theta}$, hanno origine modi risonanti nella deformazione elicoidale della colonna di plasma che giocano un ruolo essenziale nell'autosostenimento del plasma stesso.

Lo studio si basa su dati principalmente prodotti da una diagnostica denominata Neutral Particle Analyzer (NPA) che misura l'energia dei flussi di particelle neutre generati da processi di scambio carica all'interno del plasma. Grazie a questa diagnostica é stato possibile studiare la variazione dello spettro energetico della funzione di distribuzione degli ioni sotto perturbazioni. In particolare, l'analisi si é concentrata sugli effetti dei processi detti di riconnesione magnetica spontanea che caratterizzano i plasmi confinati in configurazione RFP. Tali processi avvengono per un rilassamento della configurazione magnetica tramite un riarrangiamento della topologia delle superfici magnetiche. E' noto, anche in ambito astrofisico, che tali processi di riconnesione magnetica inducono una conversione di energia magnetica in energia cinetica delle particelle sebbene non sia ancora stato del tutto chiarito quali siano i processi fisici a tale conversione associati. Tali fenomeni risultano di particolare rilevanza in esperimenti dedicati alla fusione nucleare poiché possono rivelare la presenza di meccanismi di riscaldamento ionico addizionali rispetto a quelli puramente ohmici, in grado di favorire il raggiungimento delle condizioni necessarie al processo di fusione stessa. L'analisi, inoltre, é volta alla comprensione e alla caratterizzazione degli effetti locali della dinamica riconnettiva sulla temperatura ionica.

Un primo studio sull'influenza dei modi risonanti sui flussi di particelle neutre e sulla temperature ionica ha confermato il ruolo necessario di queste perturbazioni nella generazione di processi riconnettivi. E' stata anche verificato l'effetto locali degli eventi riconnettivi sulla temperatura media. Infine, questo lavoro ha permesso di analizzare la dinamica nel tempo della temperatura, evidenziando un chiaro trasferimento di energia tra gli ioni sovratermici, per primi accelerati dal processo, e gli ioni termici.

Abstract

This thesis task is addressed to study ionic temperature dynamics inside magnetic confined plasmas of nuclear interest produced in the RFX-mod experiment. The considered magnetic confinement configuration is the so called Reversed Field Pinch (RFP), in which the direction of the toroidal magnetic field \mathbf{B}_ϕ is reversed near the edge of the chamber in which the plasma is contained. In such a configuration, for rational values of the safety factor $q(r) = \frac{rB_\phi}{RB_\theta}$, resonant modes in the helical deformation that play a fundamental role in plasma self-sustainment arise. The work is based mainly on data obtained throughout a diagnostic called Neutral Particle Analyzer (NPA), that measures the energy of neutral particles fluxes generated by charge exchange process inside the plasma. Thanks to this diagnostic it has been possible to study changes of the energetic spectrum of the ion distribution function when under perturbations. In particular, the analysis is focused on the effects of spontaneous magnetic reconnection processes which characterizes plasma confined in RFP configuration. It is known, also in astrophysical branch, that such a process of magnetic reconnection causes a magnetic energy conversion into kinetic energy of particles, even if it is not yet clarified what are the physical processes related to this changeover. These phenomena result to be of special relevance in nuclear fusion dedicated experiments since they may reveal the existence of ion heating mechanisms in addition to those purely ohmic, able to favor the reaching of the needed conditions to nuclear fusion process itself. Furthermore, the analysis is addressed to the comprehension and the characterization of local effects on ion temperature by the reconnective dynamics.

A first study on resonant modes influence over neutral particles and ion temperature has confirmed the needful role of these perturbations in generating reconnective processes. Also the local effect of reconnective events over the mean temperature behaviour has been verified. Lastly, this work gives informations on the temperature time dynamic, highlighting a clear transfer of energy between non-thermal ions, that first are accelerated by the process, and thermal ions.

Contents

1	Introduction	3
1.1	What is a plasma	3
1.1.1	Plasma parameters and orders of magnitude	3
1.1.2	Magnetohydrodynamics	4
1.2	Experimental environment	5
1.2.1	Plasma confinement	5
1.2.2	RFP peculiarities	6
1.2.3	Magnetic reconnections	7
1.2.4	Astrophysical interests in reconnections	8
1.2.5	Diagnostics	9
1.2.6	NPA: how it works	9
2	RFX shots and characteristics	11
2.1	RFP shots	11
2.2	Data analysis	11
3	Study of magnetic reconnection effects	15
3.1	Mean behaviour of parameters in RFP	15
3.2	Flux global behaviour	18
3.3	Local behaviour	20
3.4	Ion temperature behaviour	21
3.4.1	Toroidal arrangement	21
3.4.2	Locked mode effect	22
3.4.3	Modes influence on temperature	24
3.4.4	Particle distribution function	25
4	Ion heating and energy balance	27
4.1	Flux dynamics	27
4.2	Ion temperature and energy exchange	28
5	Conclusions	29

1 Introduction

1.1 What is a plasma

1.1.1 Plasma parameters and orders of magnitude

Labelled as the fourth physic state of the matter, a plasma is a ionized gas where particles show a collective behaviour. Since it is a gas, it has thermal properties such as collisionality that ease it to flow under pressure gradients and to keep a maxwellian distribution, for what concerns particle velocities. But, as long as a not negligible fraction of particle is ionized, it displays several complex dynamics related to electromagnetic interaction with external sources and the fluid itself. One fundamental feature of a proper plasma is its *Quasi-neutrality*, which means that electron density n_e and ion density n_i are very similar to each other. This property is ensured whenever $\lambda_D \ll D$, where λ_D is the so called *Debye length*, defined as the distance such that the electric potential $V(r) = V_0 e^{-\frac{r}{\lambda_D}}$ decreases to $\frac{V_0}{e}$. It is the length the characterizes the screening of the plasma with external matter. The density range covered by the many kind of plasma is huge, from $n \sim 10^6 m^{-3}$ (interstellar gas) to over $10^{32} m^{-3}$ in stars core.

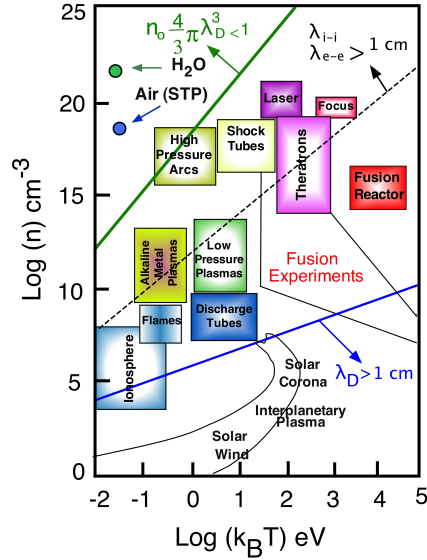


Figure 1.1: Various kind of plasma at different density and temperature

Plasmas need also to have a quite low collisionality. The physical quantities involved to describe this request are the electron plasma frequency ω_p , that is $\sqrt{\frac{n_e e^2}{\epsilon_0 m_e}}$, and the collisional frequency ν_c , so that:

$$\omega_p > \nu_c$$

Last but not least, averages must be meaningful, to treat it statistically, so a sphere with a radius equal to a Debye length should contain a great number of particles.

Typical plasma parameters are summarized in the table below [5].

Plasma	Density [m^{-3}]	Electron ω_p [Hz]	T_{e-} [eV]
Fusion reactor	10^{21}	$3 \cdot 10^{11}$	10^4
Flame	10^{14}	10^8	0.1
Solar wind	$5 \cdot 10^6$	10^4	10
Glow discharge	10^{15}	$3 \cdot 10^8$	2

1.1.2 Magnetohydrodynamics

The very appealing consequence of the existence of this state of matter is the possibility to force a gas to reach good conditions for fusion reactions. In order to get these reactions, the product $nT\tau$ has to be greater than $3 \cdot 10^{21} keVs/m^3$ [12], being τ the confinement time. Such a request is easily satisfied inside the Sun, for its gravity is so high that n in its core is over $10^{24}m^{-3}$ [9]

Of course fusion cannot be reached in this way in a laboratory, so we have to get confined plasma for long periods of time, focusing on an appropriate τ . In this sense it is needed an optimal plasma confinement. Anyhow, the gases to be used must be He, T, D or H, whose cross sections for fusion are shown in the chart below (1.2), and whose binding energy are useful to reactors.

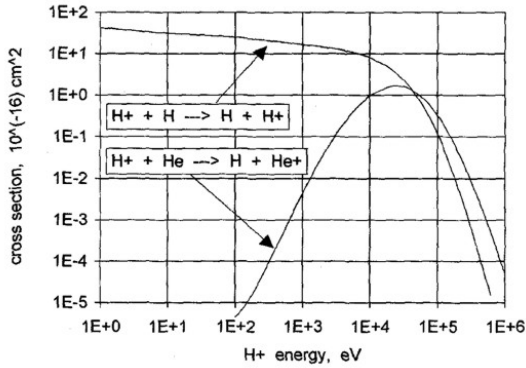


Figure 1.2: H and He charge-exchange cross sections

A plasma is, at least, composed by electrons and one species of ions, so to describe its peculiar way of interact, the easiest used theoretical model is the single-fluid Magnetohydrodynamics (from here on MHD). Let's say M the ion mass and n the density (quasi-neutral density implies it is almost the same for electrons and ions). From electron and ion continuity and motion equations, we get to a single fluid equation of motion:

$$nM \frac{\partial \mathbf{v}}{\partial t} = \mathbf{j} \times \mathbf{B} - \nabla p$$

where \mathbf{v} is the fluid velocity, \mathbf{j} the current density, \mathbf{B} the external magnetic field and p the total pressure.

Manipulating this equation one finds out a *generalized Ohm's law*, that with the due approximations appears as:

$$\mathbf{E} + \mathbf{v} \times \mathbf{B} - \frac{\mathbf{j}}{\sigma_{el}} = \frac{\mathbf{j} \times \mathbf{B}}{ne} - \frac{\nabla p_e}{ne}$$

Together with Maxwell equations and the fluid continuity equation, that is $\frac{\partial(nM)}{\partial t} + \nabla \cdot (nM\mathbf{v})$, they describe the plasma as a single fluid whose current is due mainly by electrons and its mass almost due by ions. Ideal MHD is obtained reducing the Ohm's law, thanks

to approximations, to $\mathbf{E} + \mathbf{v} \times \mathbf{B} = 0$.

Stationary settings, in which we are interested since they imply the plasma confinement, come out from ideal MHD when there is no time dependence. Substituting Ampère's law into equation of motion, one finds out another equation called *Induction equation*:

$$\nabla \left(p + \frac{B^2}{2\mu_0} \right) - \frac{(\mathbf{B} \cdot \nabla) \mathbf{B}}{\mu_0} = 0$$

This equation leads the equilibrium between total pressure and magnetic field tension.

In order to confine the plasma kinetic pressure must be balanced by magnetic tension so, whenever happens a perturbation that messes up this balance, an instability may be generated. The safety factor, defined as $q(r) = \frac{rB_\phi}{RB_\theta}$ where r and R are respectively the poloidal and the toroidal radii, has a specific value for each isobaric surface and, therefore, it needs to satisfy a restrain. In a toroidal symmetry a perturbation is characterized by a periodicity that may be express throughout an appropriate wave vector \mathbf{k} . It can be demonstrated that most of the unstable modes are resonant, that is: $\mathbf{k} \cdot \mathbf{B} = 0 = \frac{m}{r}B_\theta + \frac{n}{R}B_\phi$. So surfaces where $q = -\frac{m}{n}$ are called resonant [3]. Hereon I will refer to modes as the perturbations which has a periodicity which satisfies the resonance condition.

1.2 Experimental environment

RFX-mod (Reversed Field eXperiment) is the actual largest toroidal experiments studying fusion plasma confinement in *Reversed Field Pinch* configuration ($R = 2$ m, $a = 0.259$ m the torus radii). Plasma current can be up to 2 MA. It can also work as a low plasma current tokamak.

1.2.1 Plasma confinement

How shall we confine a gas keeping it at high temperatures in the core (for the edges must interact with the container and cannot be so hot)? Well known ways to do that is to make it linger in a magnetic field which, in many experiments, has a toroid-like shape. Three configurations are of great interest, all of them based on a *screw-pinch* shape of the B field, consisting of a toroidal field B_ϕ overlapped to a poloidal one B_θ :

- i. Stellarator is a configuration for which the reactor may work continuously and where plasma has, in principle, a perfect stability.

Its confinement is guaranteed by the external, and completely user-controlled magnetic field. Unfortunately, even if it has the most stable configuration, it needs a huge additional heat from the laboratory so there is much energy to be spent on it to make it work properly. Its symmetry is not exactly toroidal, for it has to give a precise periodic rotation of the plasma in the poloidal direction over a toroidal period, and it has to be almost perfect, not to generate instabilities. For this reason, the coil system has to be very precise and every coil is different from one another, so the stellarators are hard to build.

- ii. Tokamak is a configuration in which the symmetry is exactly toroidal and the B_ϕ field caused by the plasma itself is slightly free. Both in Stellarator and Tokamak, the toroidal field keeps its verse in the whole vacuum chamber. That means that the safety factor at the edge has to be greater than 3 to make it stable. For what concerns tokamaks $B_\phi < 10B_\theta$ in RFX. This condition, since the efficiency parameter β is usually small, means that most of the energy put into the plasma is used to make it stable.
- iii. RFP is a configuration with the same geometry of tokamaks, but while in tokamaks the magnetic field is close to a z-pinch and it has the toroidal field keeps its sign in the whole

chamber, in RFP it reverses near the edge.

The safety factor here is less than one and decreases with the axial distance until it becomes negative near the edge. Unstable modes appear where $q(r)$ is a rational number, that we can write as $\frac{m}{n}$, where m is the number of poloidal mode and n the toroidal mode number. It is peculiar that while the whole belt from 0 to 3 displays great instabilities, when q at the edge is negative the configuration finds a new stable equilibrium.

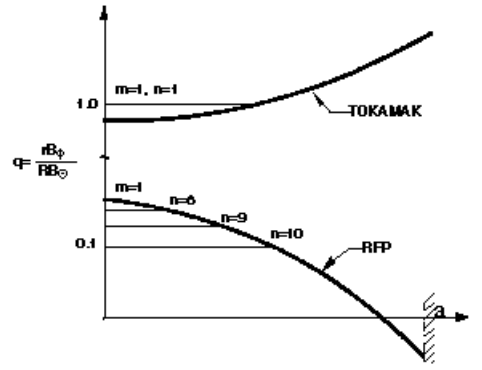


Figure 1.3: A typical safety factor for tokamaks and RFP, with $m=1$ resonances highlighted at various, at various n values

1.2.2 RFP peculiarities

Confined plasmas instabilities can be due to two kind of triggers: pressure or current gradients. Inhomogeneous pressure triggers *pressure driven instabilities*, while inhomogeneous current triggers *current driven instabilities*. A kind of pressure driven instabilities is the *Sausage*, in which the plasma column tend to interrupt where pressure is lower for magnetic and kinetic pressure are not balanced. A kind of current driven ones is the *Kink*, for which the plasma column curvature grows if not perfectly null. RFP's instabilities of interest are the so called *Tearing instabilities*. These happen when current sheets cross each other, due to reconnection. Multiple reconnections lead the creation of magnetic isles that separate from one another and overlap, so that this instabilities grow. All the previous addressed instabilities bring the configuration to collapse, but tearing modes are found to be involved in a *Dynamo* process that keep RFPs stable longer than an only resistive plasma. Indeed the dynamo effect produces an electric field parallel to the externally controlled one, so that they add up and keep the plasma current. MHD models concerning this phenomenon distinguishes between two systems in which should appear a dynamo. One, not observed yet, is the *single helicity state* (SH), where only one instability generates the dynamo. The other one, due to many instabilities overlapping, is the *multiple helicity state* (MH). Actually it has been observed a third state called *Quasi-single helicity* in which one mode, lets say $m = 1$ $n = n_0$ prevails, but many of the others exist anyway, with a low amplitude [3,4] all rotating toroidally. RFX prevailing mode is $m = 1$ $n = 7$ (1.4).

Overall, modes periodicity and rotation result in many helical deformation of the magnetic surfaces [4]. Thanks to toroidal geometry their poloidal sections are bean-

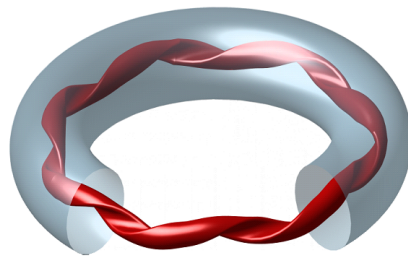


Figure 1.4: $m=1$ $n=7$ resonant mode distortion of magnetic surfaces

shaped (fig.1.5.a) and each perturbation rotate with different velocities, overlapping each other and interfering. It is well defined the phase of resonant modes, all referred to the same offset. In this way it is possible to study modes relative phase and instabilities rotation.

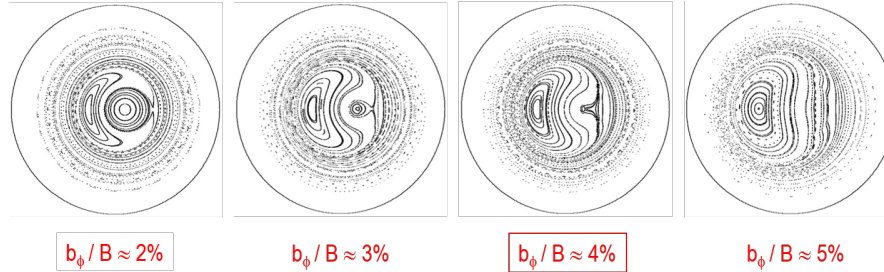


Figure 1.5: Magnetic field lines deformation poloidal shape due to resonant modes. The figure show how a perturbation (the bean shape magnetic isle) become a new equilibrium overwhelming the original shape of the magnetic surfaces

1.2.3 Magnetic reconnections

The ideal MHD model is based on the non-collisional plasma hypothesis, that obviously simplify the work, but cuts out many phenomena. In fact ions are supposed to rotate around their giration centre keeping about a Larmor radius of distance and never having any chance to switch magnetic force line, thank to the so called *Alfvén theorem*. Indeed collisions mess up this ideal coherence and let ions continuously switch between one line to another. The switching allow the magnetic lines, which are locally frozen together with the particle orbits, to cross each other and *reconnect* creating, once fragmented, two new lines, actually bonded in a unified closed line (or many lines depending of how many reconnections happen).

It is a process that takes a very small time but may be sufficiently efficient to allow huge energy transfers inside the plasma. Actual models are based on the hypothesis that reconnections are the main responsible of solar superficial events like *coronal mass ejections* (CME) and *solar flares*. Simulations through these models don't fit the experimental lapse by many order of magnitude¹.

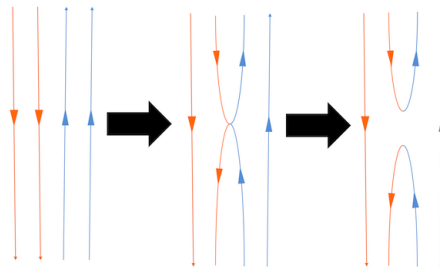


Figure 1.6: How field lines recombine in a reconnection process

Since locally the topology change brings a new equilibrium configuration and so the \mathbf{B} field has lower energy after a reconnection, some energy must have been transformed into heat or

¹Solar flares take usually a lapse of minutes or hours, while simulations point out a lapse of years

any other kind of energy, so we must seek for particle acceleration processes when reconnections happen. The process starts when lines get closer to each other: in this way an intense field gradient is generated and, consequently, local *current sheets* are produced [3]. This force the plasma to behave even less similar to an ideal MHD plasma. Forces that permit the exchange of energy between the magnetic field and the particles are coupling forces in term of \mathbf{B} and \mathbf{j} . Theoretical models about reconnections are not yet complete and not yet they can describe accurately the dynamics involved. Neither they can point out how much is the efficiency of the energy exchange during the particle acceleration nor their time orders of magnitude. It is even hard to understand the relations between local plasma parameters. This is what this thesis meant to find out from the data, throughout the study of plasma temperature. The search involved an analysis of many RFP shots sharing some average parameters. A detailed explanation of the criteria used to select what kind of shot where to consider can be found in section 2.

1.2.4 Astrophysical interests in reconnections

Magnetic reconnections happen frequently in the Sun and since they seem to be involved in CME and Solar Wind production, astrophysics take them in great interest. New discoveries about reconnections may show new interesting features about cosmic events related to them.

The sun surface is extremely turbulent and swarms with electromagnetic perturbations on various scales. The most powerful ones are the so called solar flares, that are harsh and continuous spectrum emissions, therefore related to particle acceleration. They happen impulsively on temporal scales of minutes or, at least, hours, emitting up to almost 10^{32}erg .

Sometimes flares are related to considerable matter ejections (CME). This explosive phenomenon may be involved in solar crown heating which, due to not yet clear reasons, has temperatures 10^3 times higher than those of the surface. According to Parker's model these kind of events, but at a lower scale (*nanoflares*), should be the source of coronal heating, rather than ordinary flares. In fact ordinary flares, even if very energetic, are not frequent enough to explain the heating. Reconnection events happen also on the earth magnetopause ² permitting ions to penetrate the atmosphere and give birth to auroras. State of the art satellites have recently been approved to lurch an in-situ study of the solar weather and the environment interested by the activity of the sun. To cite a few, considerable data should be collected by MMS (NASA) [1] and the Swedish THOR (ESA) [11].

²region where the magnetosphere meets the solar magnetic field

1.2.5 Diagnostics

RFX-mod vacuum vessel is equipped with 96 Langmuir probes arranged over 48 toroidal positions which compose an *Integrated System of Internal Sensors (ISIS)*, able to measure the toroidal magnetic field \mathbf{B}_ϕ .

\mathbf{B}_ϕ field values, measured with ISIS, permit to obtain the toroidal position (Φ) of magnetic perturbations and, finding out their periodicity, each resonant mode phase with respect to the same poloidal offset. In particular, we are interested in toroidal position of reconnective events. Further on, all the figures showing behaviours as a function of time and toroidal position Φ are addressed to compare the NPA data reading recorded at the reconnection moment with the effective position of the reconnection itself.

In fig.1.7 there is an example of ISIS data reading of \mathbf{B}_ϕ value, where at the highlighted position and time a reconnection has been recognized.

Even resonant mode 1/7 phase is of great importance since it can underline if the bean-shaped perturbation is in front of the NPA or in a different poloidal position during a reconnection. In the same way, the poloidal position of the locked mode (*Lockpos*) has been found and used for the analysis.

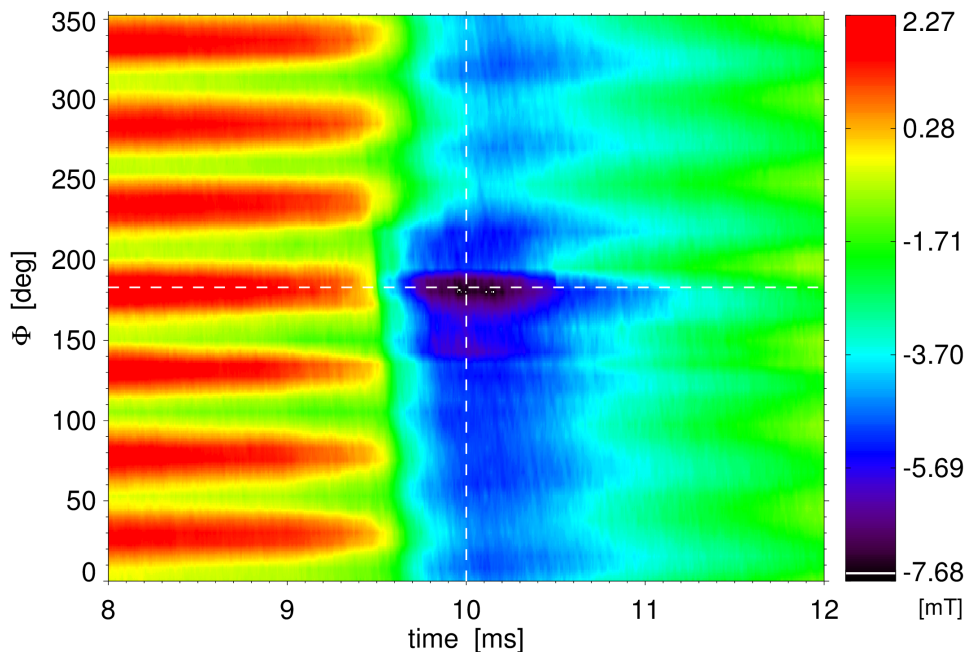


Figure 1.7: An example of magnetic field measure by ISIS. The white lines highlight where and when the reconnection, coinciding with a field crash, happened.

1.2.6 NPA: how it works

To estimate the ion temperature inside the core not many ways are available. One way might be through spectroscopy, but since the ionized gas (usually H or D) doesn't have any electron orbital occupied, there is no energy transition to see and therefore no Doppler effect on the spectral lines. Sure not every particle is ionized at the edge, but in the core the energy transmitted to atoms are easily greater than the minimum for ionization. To deal with it, we have the luck of the existence

of a process called *charge exchange* for which cold neutrals, that no field has interaction with, can impact with high energy ions leaving them their shell electrons without changing momentum. Consequently high energy neutrals are shot out of the vacuum chamber, letting them to carry out information about ion temperature in the core. The main source of cold neutral is naturally the plasma edge, but an external source can be anyway used instead.

Once neutrals leave the vacuum chamber, they have to be revealed. At this purpose a Neutral Particle Analyzer (NPA) is equipped [8]. It works as like as a mass spectrometer: neutrals cross a cold plasma to get their charge back, through charge-exchange collisions, and the ion beam obtained is driven through a magnetic field perpendicular to its line of flight. Here Lorentz force acts to separate different energy ions. To know how many ions of which energy have been dumped, 11 *channeltrons*, which are electron multipliers are placed as shown schematically in figure 1.8(a). Figure 1.8(b) describes how NPA works: the neutral particle flux cross a stripping cell to obtain a charged particle flux.

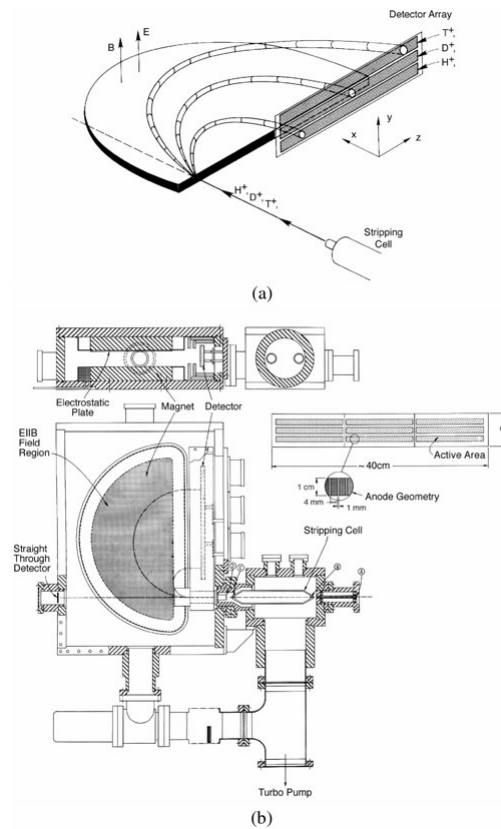


Figure 1.8: NPA scheme and principle. The dispersion is given by $E//B$

2 RFX shots and characteristics

2.1 RFP shots

Not all the shots recorded since RFX-mod start to now could be used. The database of data consists of 357 RFP shots showing a good behaviour. They all needed to have same features. A first limit is due to equipment failures or lack that force to pay attention whether the diagnostics worked well. In every shot considered for the analysis the used gas was H, since it brought more statistics.

Plasma current (I_p) range was huge: from 200, to nearly 2000 kA of top value. But since I_p has such a great spreading over time, reconnections used to study properties related to a local dynamics were chosen over the I_p flat top. In the example below (fig. 2.9), we can consider as flat top the range between 50 ms and 160 ms.

Not all the shots recorded since RFX-mod start to now

2.2 Data analysis

$B_t(a)$ crashes correspond to the *reversal parameter* crashes, for it is defined as $F = \frac{B_\phi(a)}{\langle B_\phi \rangle}$. But, since the sampling time base was finer for the toroidal field, the moments of $B_t(a)$ minimum were chosen as the precise moments of when reconnections happened, instead of F minimum instants. The purpose of the main analysis is to find out the dynamics of NPA fluxes when reconnection process occurs. It needed to start from an analysis of parameters changes and global and local influences of modes perturbations on neutral production. In next sections the study is developed this way:

1. Averaged relevant plasma parameters mean behaviour;
2. Averaged fluxes global and local behaviour;
3. Study of the temperature changes due to local effects, resonant modes effects and locked mode position influence;
4. Study of particle distribution function changes due to parameters different values;
5. Study of the dynamic of energy exchange throughout fluxes and temperature timings.

The study has as main focus the ion temperature's behaviour and, in order to do this, the results are obtained through an average over the shots at the varying of meaningful plasma parameters.

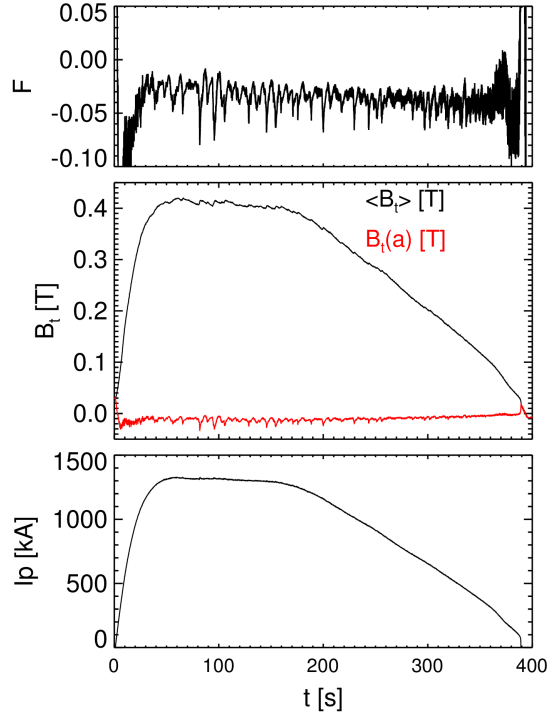


Figure 2.9: A typical time trace over a complete RFP shot of a few relevant parameters. From this charts it is possible to see that \mathbf{B} crashes correspond to F crashes

1. F , at the current flat top keeps almost constant, except for fluctuations, even crashes. It is common to distinguish between shallow F and deep F. A more accurate distinction has been done, selecting F in ranges [0-0.1], [-0.1;0], [-0.2;-0.1] and [-0.4;-0.2];
2. I_p , measured just before the crashes, was framed into ranges [200;600], [600;1000] and [1000;2000] kA.

As the chart below shows (fig. 2.10)), n_e , depending on I_p , never exceeds a limit called *Greenwald limit*. It is interesting to consider density and current related, examining the mean behaviour through a classification in Greenwald limit percentages. The actual percentage splittings taken into account are 0.20 and 0.40. The analysis are based on n_e/n_G intervals delimited by these two splitting, so they are: [0;0.2], [0.2;0.4] and [0.4,1].

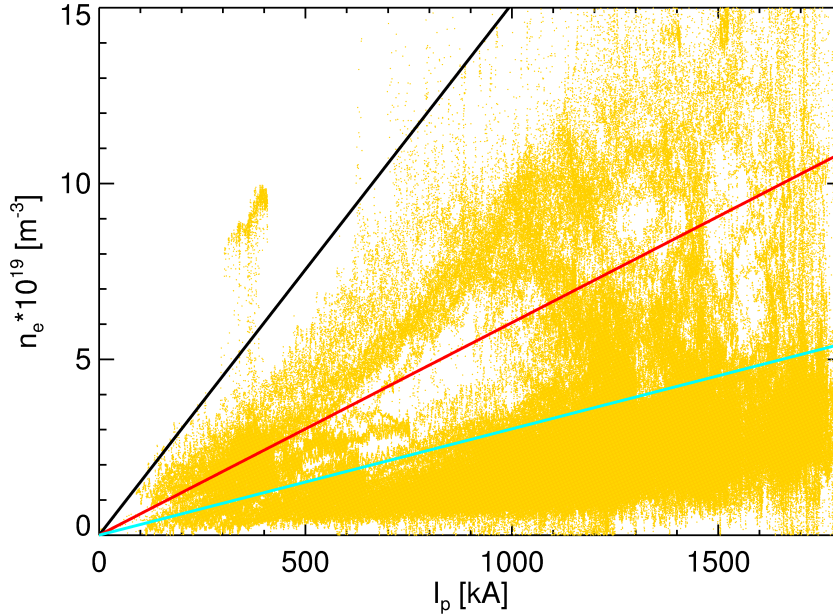


Figure 2.10: Electron density n_e depending on I_p . It never exceeds the Greenwald limit, represented in the chart as the straight line with higher slope. The black line represents the Greenwald limit, where $n_e/n_G = 1$. The other two lines correspond to $n_e/n_G = 0.4$ (red line) and $n_e/n_G = 0.2$ (green line).

The spectrum of the outgoing flux gives us informations about temperature. In a RFP the particle distribution function is almost maxwellian except for a high energy non-thermal tail [7]. Said $C(t)$ the flux of outgoing neutrals, since the distribution function may be written as $C(E) = C_0 e^{-\frac{E}{T} + \gamma E}$, then at least the temperature of low energy ions can be estimated throughout an exponential linear regression in the energy range just before a *knee* due to the non-thermal tail. Expressly, the best behaviour range appeared to be from 1334 eV to 2424 eV. To check whether the knee location was well fixed, a preliminary analysis has been done this way:

1. two different regression were traced. One from the two NPA fluxes associated to the lowest energies, for slow ion temperature, and one from the highest two NPA channels, for the high energy tail.
2. The intersections were found
3. Then the closest energies to the intersections were chosen as the knee actual position.

Mostly, knees were found near 2424 eV. Both for thermal and non-thermal ions, the flux has been interpolated via a linear trend:

$$\log(C) = a + b \cdot E$$

So temperature is estimated as $-\frac{1}{b}$. I'll refer to the two temperatures as T and T^* to distinguish between the one obtained interpolating low energy neutrals fluxes and the one obtained, in the same way, interpolating the high energy fluxes. T^* is not strictly a temperature, even it has the same dimensions, for it describes a non maxwellian population of ions. It is useful to give it a similar name, only to understand better the non thermal tail spectrum behaviour.

As said previously, 11 NPA channels were used, but we found out that the 5th and the 9th channels had troubles so they were to be ignored. Actually also the very first channel was to be ignored.

Another kind of analysis that concerned how $m=0$ and $m=1$ poloidal modes interfere has been done. It happens, as consequence of the interaction of the plasma column with the shell [2], that $m=0$ and $m=1$ modes overlap themselves, setting up a stationary deformation toroidally locked to the wall, and therefore called *Locked mode*. Its toroidal position may underline a role of the modes in the dynamics, since the plasma-wall interaction is fiercer there [10] and so displays a greater local production of cold neutrals. For this kind of search there was no need to establish a current flat top so, instead of narrowing down only to the flat top intervals, the whole shot developments have been taken into account.

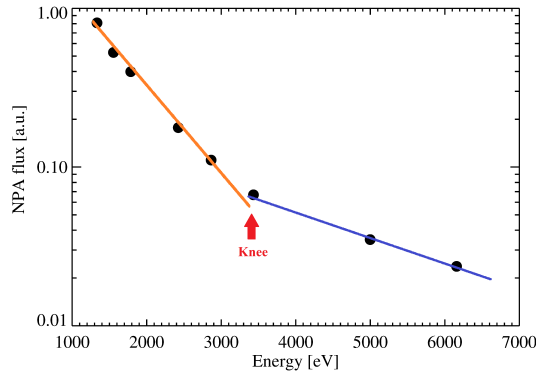


Figure 2.11: An example of ion distribution function. The orange line represents an interpolation of low energy channels which gives thermal temperature. The blue one gives a similar result for high energy ions. The knee of the distribution is highlighted by the red arrow.

3 Study of magnetic reconnection effects

3.1 Mean behaviour of parameters in RFP

Around the crash instants, relevant plasma quantities show changing in a few ms. Taking into account this strict range, the whole analysis is done over a time window from 6 ms before the crash to 6 ms after, to let the signals return to their stationary value. Interesting parameters' behaviours averaged are shown below.

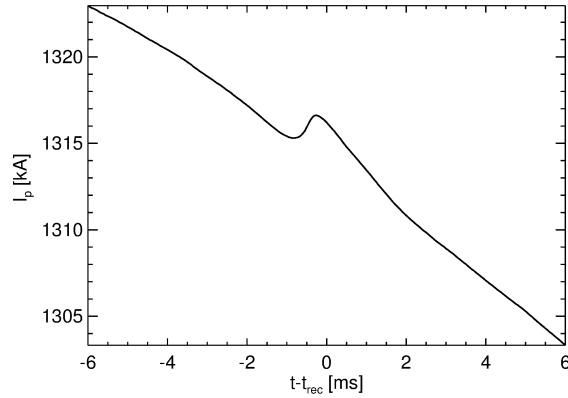


Figure 3.12: Averaged current behaviour during a reconnection

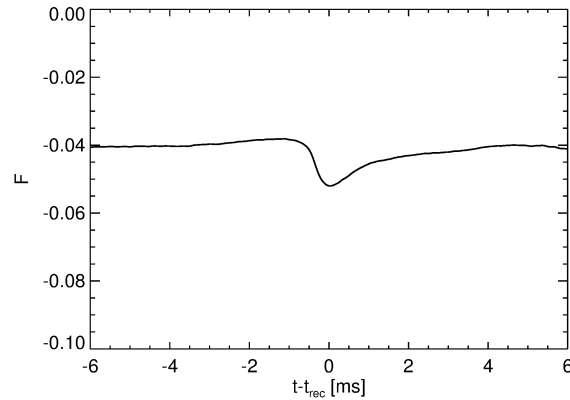


Figure 3.13: Averaged F parameter behaviour during a reconnection

It is meaningful to see how F sinks about an hundredth (fig. 3.13) while the I_p has an half kA peak (fig. 3.12). The reversal parameter displays perturbations at different scales and with various frequencies. Not all these perturbations correspond to crashes but the more intense ones. Electron temperature (fig.3.14) has the slowest changing, for it starts increasing about 4 ms before the crash and has a very smooth profile.

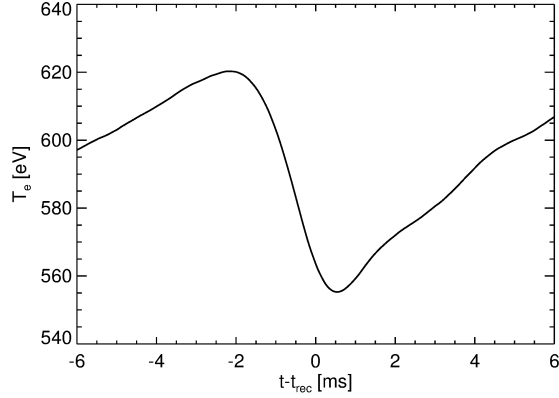


Figure 3.14: Averaged electron temperature during a reconnection

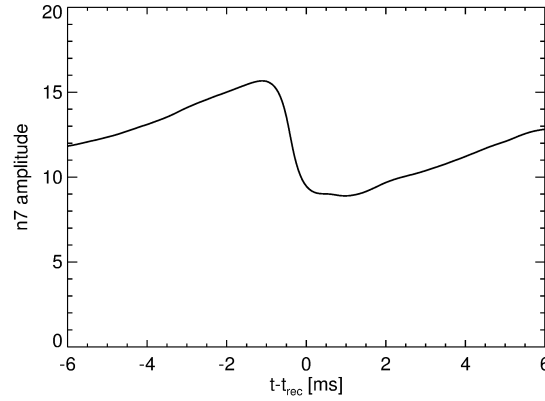


Figure 3.15: Mode $m/n=1/7$ amplitude time behaviour during a reconnection

The fact that all the quantities are smooth on average tell us statistics is good. It is good to notice that $m/n=1/7$ mode amplitude sinks during a reconnection. This is quite clear because magnetic surfaces completely change topology and modulations disappear with the previous configuration. The phenomenon revealed by the mode amplitude crash (fig. 3.15) has a considerable effect on fluxes. Picture 3.16 shows separately low and high energy fluxes just before and meanwhile the reconnection takes place, that is when the phase is not well defined. Following Spitzer's theory [6], hot plasma conductivity follows the law: $\frac{12}{\sqrt{2}} \frac{\epsilon_0^2 (\pi K_B T_e)^{3/2}}{Z e^2 \sqrt{m_e} l n \Lambda}$, with $l n \Lambda$ the Coulomb logarithm, and it is therefore proportional to $T_e^{3/2}$. Anyway the process is very fast and one should not be misled by the behaviour of T_e . Indeed electrons have higher mobility than the ions, so when a B field crash occurs, electrons follow them quickly and, since also confinement get worse, they slip out and bring thermal energy to the wall. Ions, on the contrary, don't feel the disruption immediately and appear to increase their own temperature. Electron temperature modulations, during a reconnection, is a consequence of it due to the breaking of topology, while plasma current peaks are caused by an inductive effect.

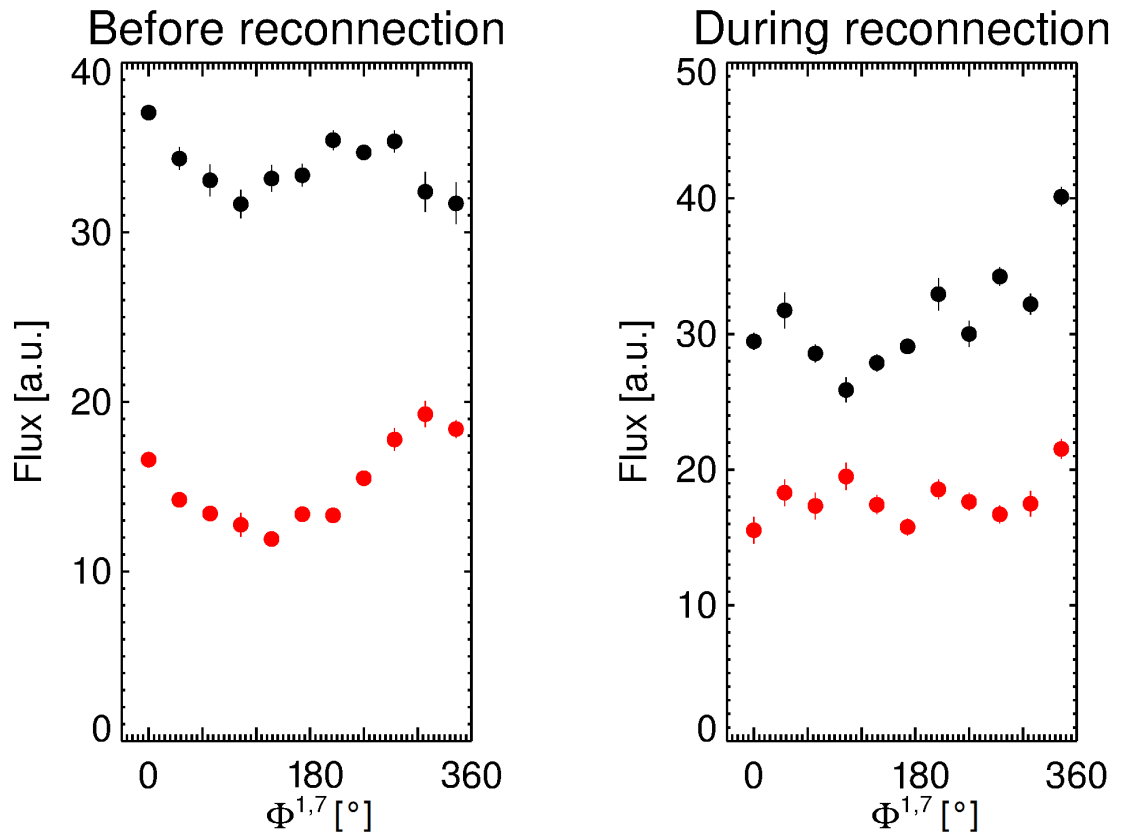


Figure 3.16: NPA flux is modulated mainly by the $m/n=1/7$ mode, so that when in phase, the outgoing flux is higher thanks to a greater local production of neutrals. The picture shows a low energy flux (black) and a high energy flux (red), before and during the reconnection.

3.2 Flux global behaviour

The first thing we see if we take an average of the fluxes recorded during a reconnection is a global decreasing, as shown in fig. 3.17. What actually happens is that low energy fluxes decrease, while high energy ones have a rapid peak (fig.3.18) . There are almost two orders of magnitude between low energy and high energy fluxes, so that the whole effect is overwhelmed by the low energy ones. Although it is an average chart, picture 3.17 suggests us what happens to the total energy. If we integrate the fluxes with their mean energy, we take a new information about the dynamics.

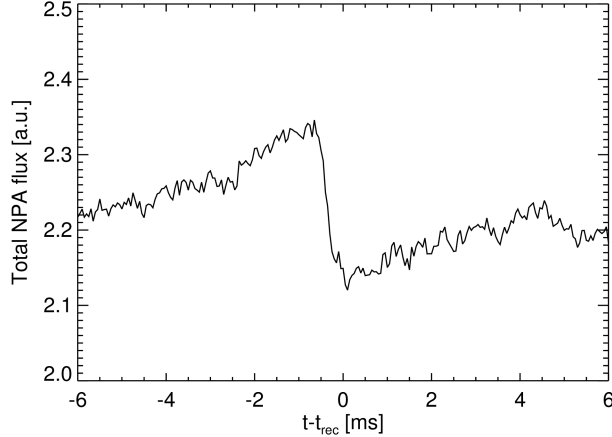


Figure 3.17: Global normalized flux behaviour

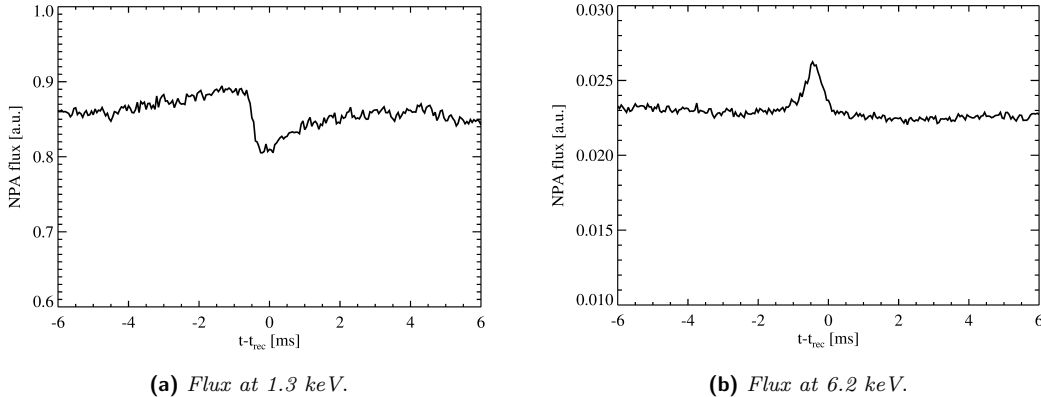


Figure 3.18: Different NPA flux at different energies. At low energy (a) a fall appear during a reconnection, while at higher energy (b) there is a peak suggesting the growth of the non thermal tail.

As shown in the pictures below, just near the knee location the energy flux behaviour, as well for particle flux (fig. 3.19), changes showing peaks instead of a fall. The total energy flux decreases at the crash, because of the minor number of high energy ions. Next pictures show also the toroidal distribution of the energy flux. Particle fluxes behaviours differ from figures 3.19 only by a scale factor, therefore useless to show. Notice that NPA toroidal angle is 277° (white line). We must keep in mind that what the NPA reveals is not directly ion temperature, ion flux

neither; then even if the total decreasing suggest somehow that energy disappears, it is related only to the neutral flux revealed.

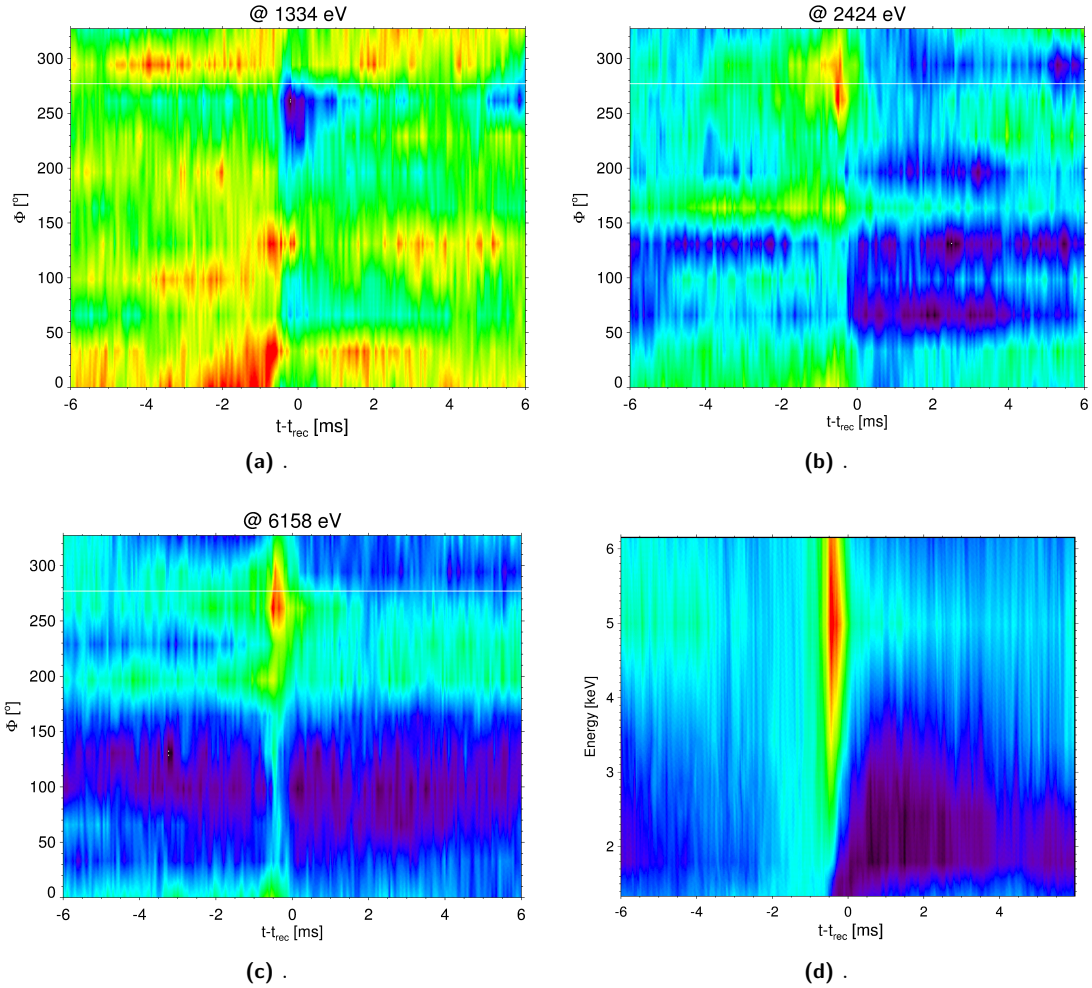


Figure 3.19: Pictures a, b and c show energy fluxes behaviour as a function of time and toroidal position (Φ) for different energy channels. The mean behaviour of normalized fluxes (picture d), depending on time and channel energy, shows also a different timing at different energies

Although the NPA reveals neutrals, the decreasing of their flux can also be due to a better confinement. In fact, even if neutrals are not confined at all, their source is strongly linked to confinement, for it is the wall itself. Whenever the field crashes, there is a reset of the unstable modes and then a change in the plasma-wall interaction. If confinement is improved then a less number of ions reach the wall with enough energy to desorb neutrals and, obviously, there are less charge exchange events. Consequently, neutral particle fluxes sink.

3.3 Local behaviour

Looking at the previous picture 3.19, we find that the reconnection acts locally. NPA has a very little solid angle of view, so that it actually reveals only neutrals coming from its position. What picture 3.19 shows is the number of particles recorded by the NPA during the reconnection varying the crash toroidal position. The toroidal position belongs to the reconnection. Therefore a local dynamic involving neutral fluxes revealed is relative only to reconnection events happening in that exact position.

So, since neutrals density changes are set near $\phi = 277^\circ$, one can conclude that reconnection acts very locally on neutrals. The meaningful toroidal range to study is then centered at 277° . It is clear that a precise analysis of flux behaviour is to be done in the range $250^\circ - 300^\circ$. This filter on the toroidal position range was used in most of the temperature analysis.

Since the analysis is well focused on local particle fluxes, also temperature must display a local behaviour, with no relevant changes elsewhere on the toroidal position.

3.4 Ion temperature behaviour

3.4.1 Toroidal arrangement

Also thermal temperature pattern show a local behaviour. Figure 3.20 shows, for low energy ions, a temperature growth, while none is found for T^* (fig. 3.20). That may mean that, since their flux is slightly increasing, the whole plasma is thermalizing.

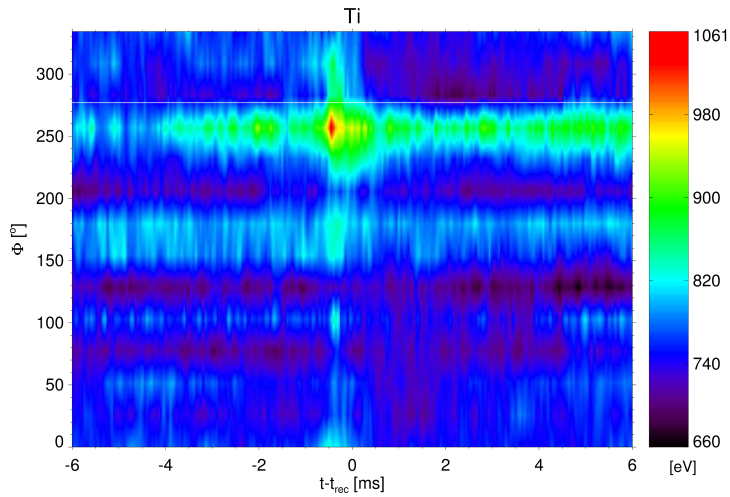


Figure 3.20: T behaviour as a function of time and toroidal angle.

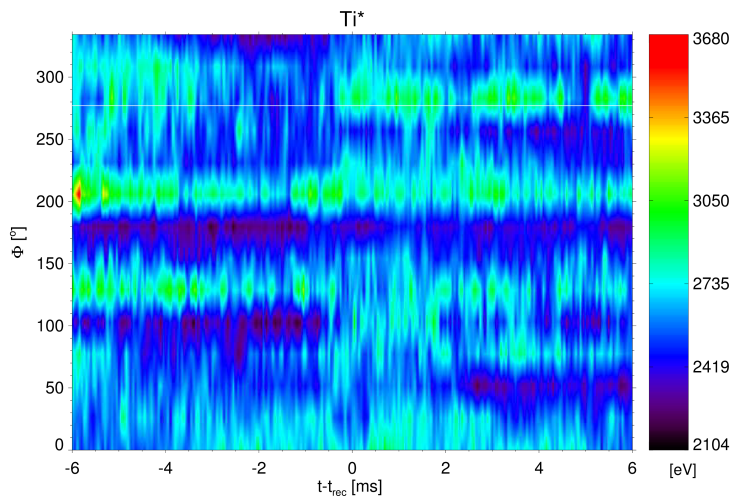


Figure 3.21: T^* behaviour as a function of time and toroidal angle

Picture 3.22 shows averaged low energy ion temperature over time, in three different intervals.

Thermal ions raise their temperature about 200 eV where reconnections happen, while they keep a mean profile elsewhere. There is not any local effect on the non thermal ion tail (3.23).

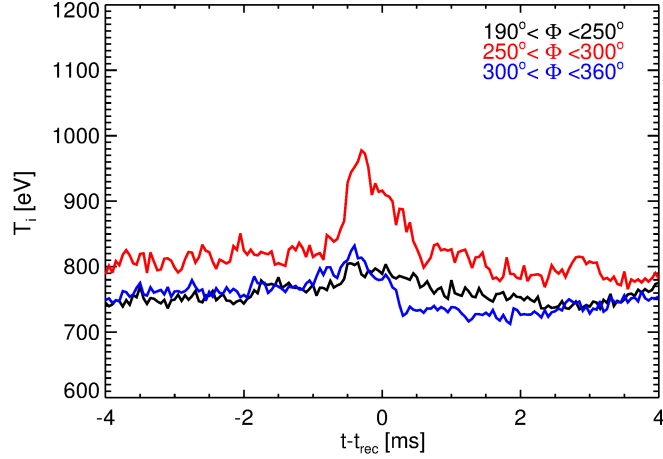


Figure 3.22: Low energy ion temperature T averaged onto three different toroidal angle ranges. The red curve belong to events caught in front of the NPA

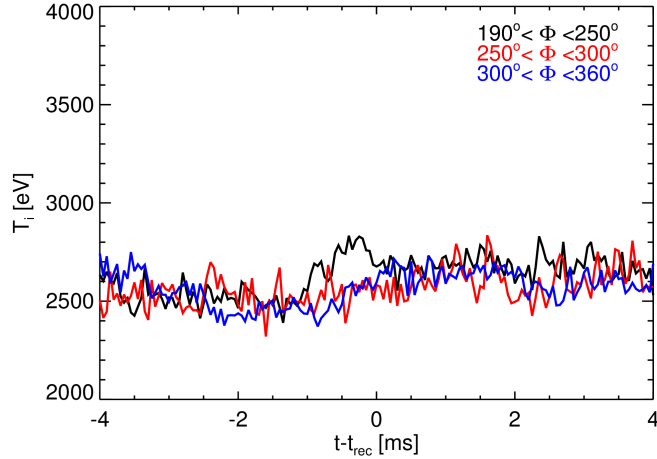


Figure 3.23: High energy ion spectrum slope T^* averaged onto three different toroidal angle ranges. The red curve belong to events caught in front of the NPA

3.4.2 Locked mode effect

As we can see from the charts 3.24 and 3.25 the analysis focused on the locked mode shows a very light effect, with high I_p both for the low energy ions and high energy ones. A modulation of fluxes does not entail necessarily a modulation of temperature. At low current, since fast ions feel better the inflection, only high energy fluxes are altered clearly. Anyway the locked mode is easily overwhelmed by the 1/7 mode at high current, consequently the effect on temperature is obviously weaker since the effect on the neutral source is weaker too.

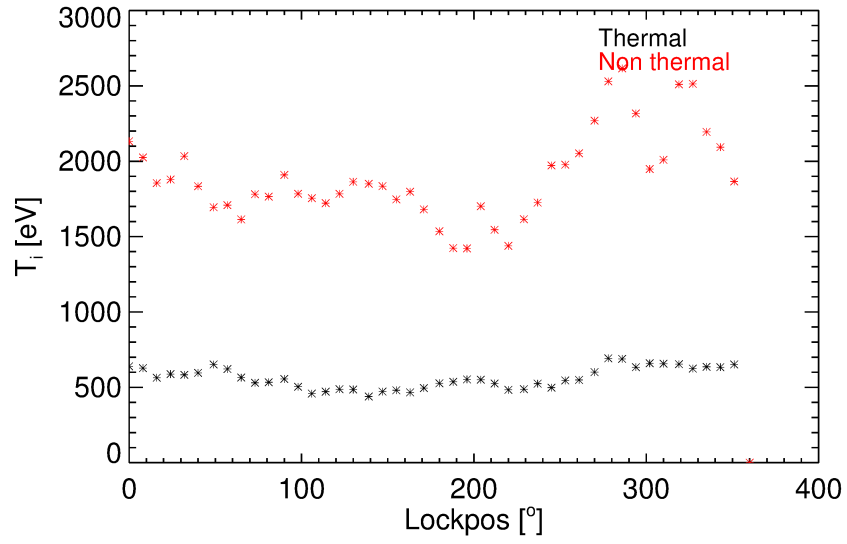


Figure 3.24: T and T^* as a function of the locked mode position at low plasma current. The black curve refers to thermal ions, while the red curve refers to the non thermal contribute.

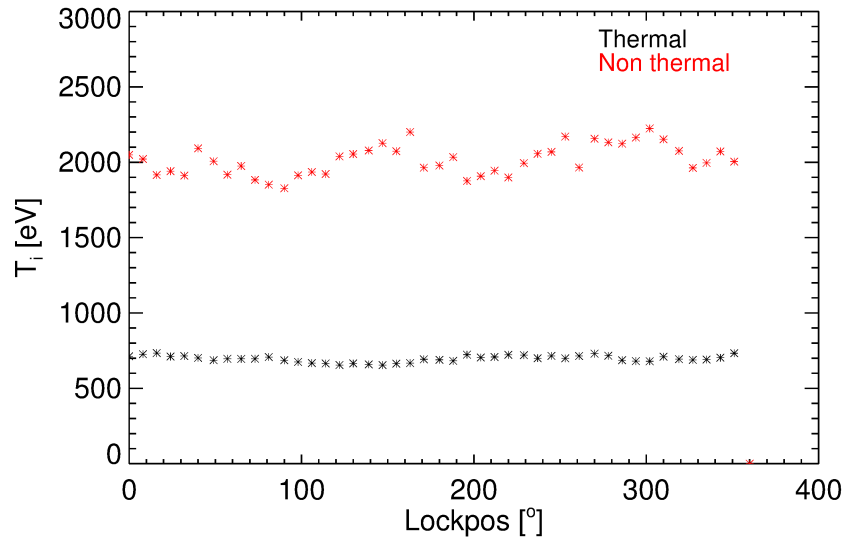


Figure 3.25: T and T^* as a function of the locked mode position at high plasma current. The black curve refers to thermal ions, while the red curve refers to the non thermal contribute.

3.4.3 Modes influence on temperature

Does the resonant mode 1/7 have any influence on temperature? It actually seems stronger than the locked mode. In this case the modulation rotates on the poloidal angle and affects neutral production and ions confinement. Thermal ions production is favored by the mode interaction with the wall, so that the distribution function is altered heavily where in phase with the mode, expressly when the bean-shaped deformation is in front of the NPA. As in the following images (fig.s 3.26 and 3.27), both thermal temperature and non thermal contribute feel the mode. The actual decreasing of T^* suggests again, but here more firmly, that a heating is happening.

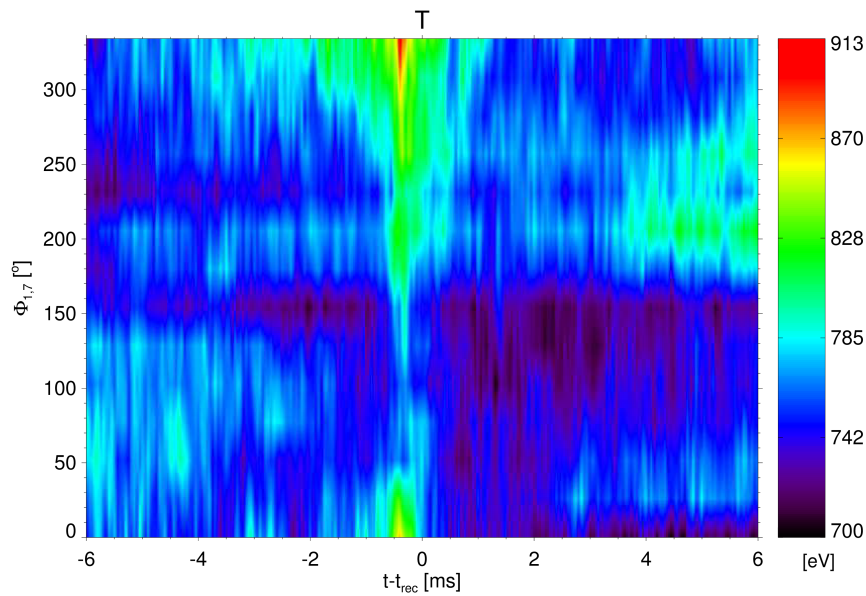


Figure 3.26: T behaviour modulation due to resonant mode $m/n=1/7$

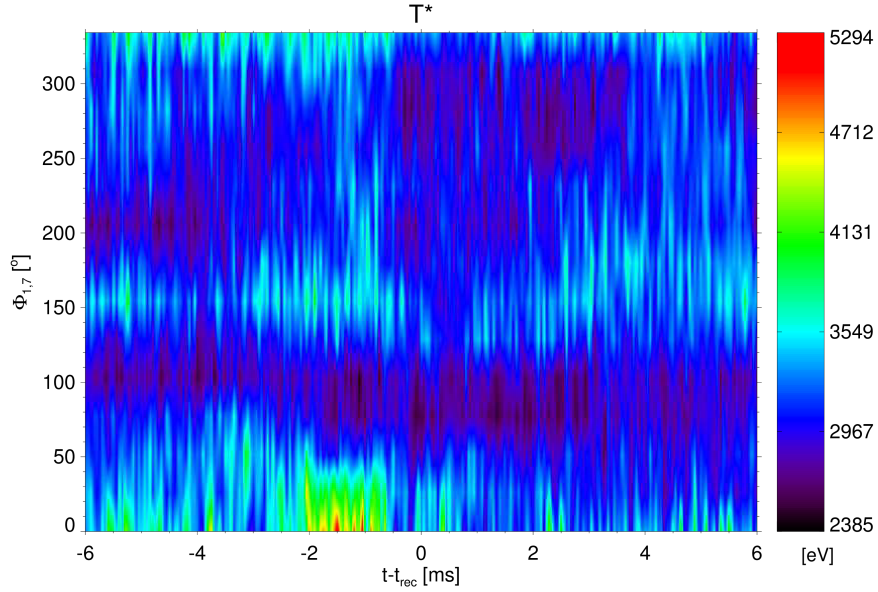


Figure 3.27: T^* behaviour modulation due to resonant mode $m/n=1/7$

3.4.4 Particle distribution function

Different electron density and current ranges bring different particle distribution functions. In particular, ion temperature seems to be lower at lower currents. Figure 3.28 show particle distributions at both different density and current ranges. Picture 3.28 (a) refers to a current range $1000 < I_p < 2000kA$, (b) refers to current range $600 < I_p < 1000kA$ and (c) refers to current range $200 < I_p < 600kA$.

The reversal parameter, instead, doesn't seem to influence much the distributions, at least in the current-density best range ($1000 \div 2000kA$, $n_e/n_G < 0.2$) (fig. 3.28.d). The only evident change is the increasing difference between thermal ions population and the non thermal tail as the reversal parameter belongs to deeper ranges.

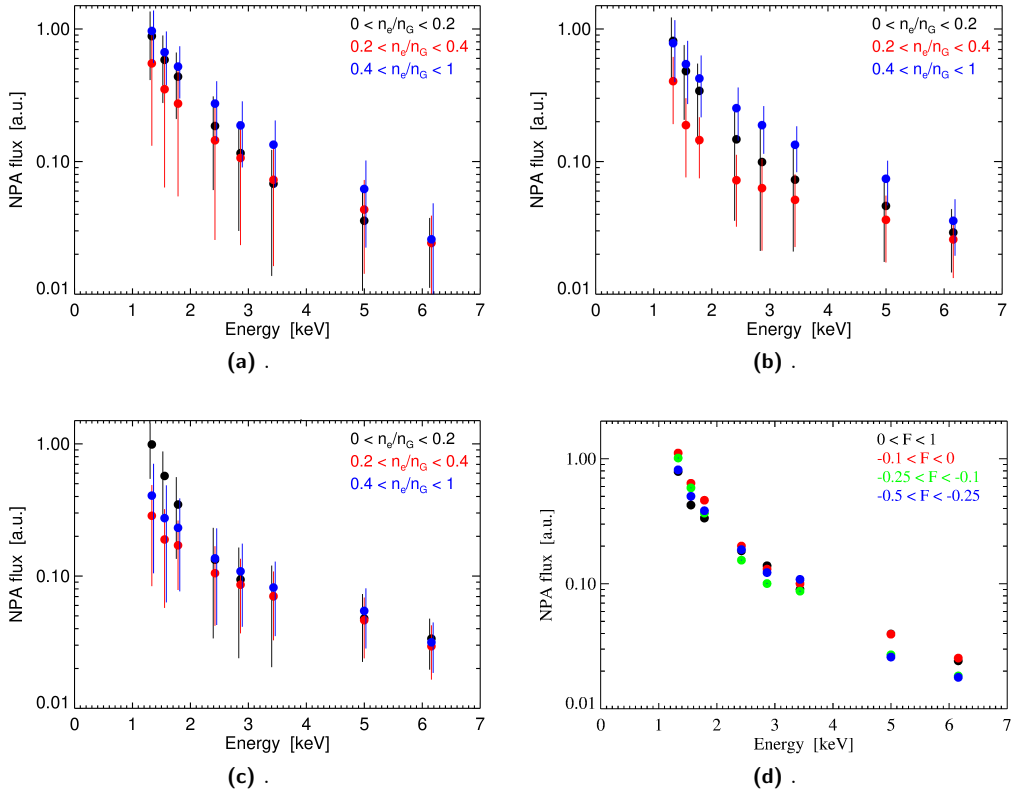


Figure 3.28: Distribution functions with error bars at different I_p (a)(b)(c), varying density ratio $\frac{n_e}{n_G}$. Distribution function at different values of F , with high I_p and low $\frac{n_e}{n_G}$ (d).

4 Ion heating and energy balance

4.1 Flux dynamics

From figure 4.29.c one learn another information: not all the fluxes change at the same moment. Here below, plotting NPA channels fluxes intensity versus their mean energy and versus time, we can see that when low energy fluxes fall, high energy ones have already started increasing.

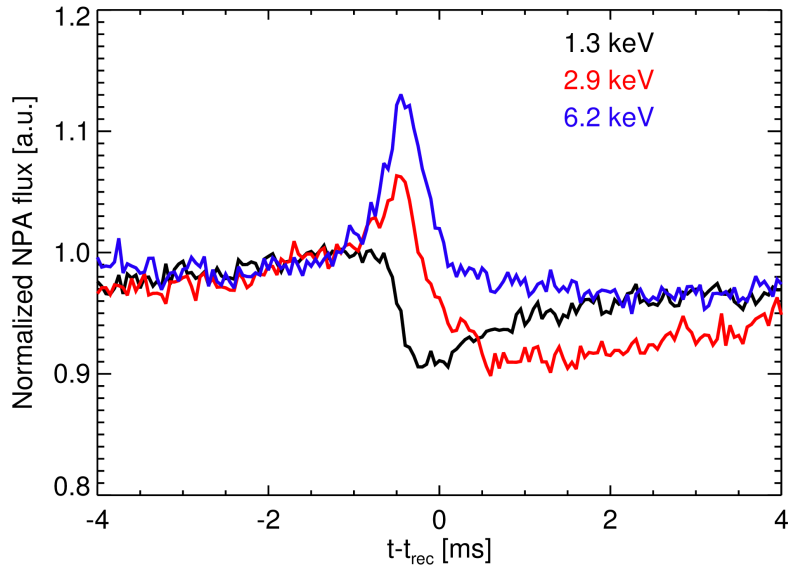


Figure 4.29: Three normalized NPA fluxes time trace compared

A better explanation of the timing in this process may be found in these next pictures: arrow heads show time verse, from just before the crash and just after (fig. 4.30). This remarkable analysis result underlines how the heating process develops, starting from fast ions. Here is normalized intensity of three NPA channels with different energy plotted versus the lowest energetic one. High energy NPA channels start growing before the lowest energy one and the time development tends to display a phase quadrature increasing the energy gap. On the other hand, they appear to be in-phase the more their energy is comparable.

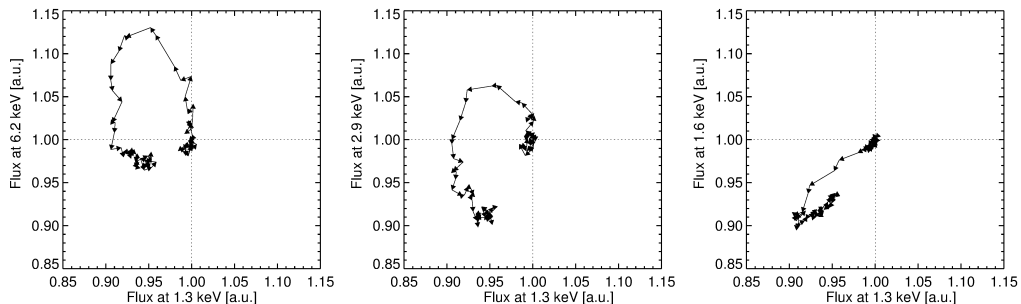


Figure 4.30: Time development of normalized fluxes compared. It tends to be a phase quadrature increasing mean energy gap, while in-phase at comparable energy.

4.2 Ion temperature and energy exchange

What happens to temperatures? The state which display a neat dynamic has high I_p and low n_e/n_G (fig. 3.28 black curve). This range has the intrinsic merit of having a better statistics (fig.2.10) but a further analysis may reveal more accurately temperature changes.

Low temperature has its maximum almost at the end of the thermal fluxes sinking, while the slope of high energy ions distribution (T^*) decreases slowly at the beginning of the process, as the non thermal flux starts increasing. At the reconnection time low energy fluxes nearly reach their minimum while high energy ion fluxes have already reached their top value. At that time, particle distributions appear to be more straight and the whole ion population more thermal. The whole effect on the distribution function, considering this time development, appears to be like a transfer of energy between particles:

1. High energy particles increase, but their mean temperature decreases, so that the knee shifts towards low energy fluxes
2. Low energy fluxes start then decreasing and their temperature increases, so that the knee comes back toward high energy ions but with a major flux intensity. At this point the distribution function is closer to a Maxwellian
3. Starting from the knee, all comes back to their average as before the reconnection.

From this result, can be deduced that the heating process starts from high energy ions, who transfer their energy to low energy ones by collisions and the plasma first warms up, then cools down.

5 Conclusions

This thesis work has been dedicated to the analysis of the neutral particles exiting the plasma produced in the RFX-mod device for the study of magnetic confinement. These particles are produced by charge exchange processes between low energy neutrals and high energy ions so that an analysis of the energy spectrum of the population of the non confined neutrals gives informations about the ion distribution function. The analysis has been focused on the data coming from a Neutral Particle Analyzer which reconstructs the neutral distribution function in the velocity space through combination of the action of electric and magnetic fields on re-ionized particles.

In the analysis I considered a large amount of data collected from a wide range of experimental conditions in terms of plasma current, equilibrium and electron density. Reversed Field Pinch discharges have been considered which are characterized by intense magnetic dynamics due to spontaneous reconnection processes that are known to be related to the release of magnetic energy in the form of particle heating.

The energy spectrum of the collected particles showed the presence of two different populations of ions: a thermal subset, whose spectrum gives information on their mean temperature, and a high energy tail that deviates from the maxwellian distribution. These two populations revealed they don't behave the same way when involved in reconnective processes, but they display heating dynamics linearly related to ion energy.

Through a local analysis in the best found range of values for plasma current and relative electron density, it has been found out that the particles fluxes generated from thermal and non thermal ions interaction with wall-desorbed neutrals follow different dynamics.

It has been clarified that a local ion temperature perturbation follows a flux local perturbation, due to the local related reconnective event. It is also a good result that the modes interaction with the wall favors neutrals production.

Reconnection influence on particle acceleration is undeniable and it is a fast local process that acts certainly increasing thermal temperature and allowing plasma to thermalize locally. The action on the high energy tail suggests that high energy ions feel easier this magnetic field perturbation. It is important to underline that it is not clear if the energy given to these high energy ions is related to a kind of temperature or is a less stochastic acceleration. However, a very neat result is that low energy ions, maybe thanks to their greater number, absorb part of the energy given to fast ions. In this way, for a brief time, the whole plasma gains in temperature.

The observation of this kind of non-ohmic heating of the plasma in RFP configuration will be eventually considered of thermonuclear interest since further studies on this topic may improve plasma confinement and more efficient ways to reach fusion conditions.

References

- [1] www.nasa.gov/mission/_pages/mms/index.html.
- [2] F. Auriemma. *Particle transport in Reversed Field Pinch plasmas*, 2008.
- [3] L. Cordaro. *Studio dei processi di riconnessione magnetica in plasmi di interesse termonucleare*, 2014.
- [4] D. Escande. *What is a reversed field pinch?* <https://hal.archives-ouvertes.fr/hal-00909102>, Nov 2013.
- [5] F.F.Chen. *Introduction to plasmas physics and controlled fusion*. Plenum Press, second edition edition, 1974.
- [6] C. Forest, K. Kupfer, T. Luce, P. Politzer, L. Lao, M. Wade, D. Whyte, and D. Wroblewski. *Determination of noninductive current profile in tokamak plasmas*, 1994.
- [7] D. Hartog. *Ion energization during magnetic reconnection in the RFP laboratory plasma*. Oct 2012.
- [8] A. Kislyakov, A. Donn, L. Krupnik, S. Medley, and M. Petrov. *Particle diagnostics*. 53, 2008.
- [9] Nasa. <http://solarscience.msfc.nasa.gov/interior.shtml>.
- [10] S.Hokin, H.Bergsaker, P.Brunsell, J.Brozowski, M.Cecconello, J.Drake, G.Hedin, A.Hedqvist, D.Larsson, A.Moller, E. Sallander, and H.H.Saetherblom. *Locked modes and plasma-wall interaction in a reversed-field pinch with a resistive shell and carbon first wall*.
- [11] A. Vaivads. *THOR Exploring plasma energization in space turbulence*. Jan 2015.
- [12] J. Wesson. *Tokamaks*. Clarendon Press, second edition edition, 1997.